Available online at www.sciencedirect.com
ScienceDirect
ELSEVIER
Electrochemistry Communications 9 (2007) 497–503
electrochemistry communications
www.elsevier.com/locate/elecom

A new flow field design for polymer electrolyte-based fuel cells

C. Xu, T.S. Zhao *

Department of Mechanical Engineering, The Hong Kong University of Science and Technology, Clear Water Bay, Kowloon, Hong Kong SAR, China

Received 3 October 2006; received in revised form 14 October 2006; accepted 16 October 2006
Available online 14 November 2006

Abstract

We present a new flow field design, termed convection-enhanced serpentine flow field (CESFF), for polymer electrolyte-based fuel cells, which was obtained by re-patterning conventional single serpentine flow fields. We show theoretically that the CESFF induces larger pressure differences between adjacent flow channels over the entire electrode surface than does the conventional flow field, thereby enhancing in-plane forced flow through the electrode porous layer. This characteristic increases mass transport rates of reactants and products to and from the catalyst layer and reduces the amount of liquid water that is entrapped in the porous electrode, thereby minimizing electrode flooding over the entire electrode surface. We applied this new flow field to a single direct methanol fuel cell and demonstrated experimentally that the new flow field resulted in substantial improvements in both cell performance and operating stability as opposed to the conventional serpentine flow field design.

Keywords: Polymer electrolyte membrane fuel cell; Direct methanol fuel cell; Water flooding; Flow field; Under-rib convection

1. Introduction

Polymer electrolyte membrane (PEM)-based fuel cells, including hydrogen fed PEMFCs and direct liquid methanol fuel cells (DMFCs), offer the tantalizing promise of cleaner electricity with less impact on the environment than traditional energy conversion technologies. However, the commercialization of PEM fuel cells is still hindered by several technological problems, among which severe water flooding of the cathode and the induced mass transport losses are critical [1–3]. Over recent decades, different fundamental issues of the PEMFC system, including the water management of the cathode, have been studied extensively [1–31].

The flow field is one of the key components of a PEMFC, which serves as both the current collector and the reactant distributor. The reactants, as well as the products, are transported to and from the cell through the flow channels. The essential requirements for the flow field are uniform distribution of reactants over the entire electrode surface and effective removal of products from the cell, to minimize the concentration polarization. To this end, different flow field configurations, including parallel, serpentine, interdigitated, and many other combined versions, have been developed [3]. It has been understood that the flow field design has a deterministic role on mass transport and water management, and thus great efforts have been made for the optimal design of flow field such that high and stable cell performance can be achieved [3–28].

Yamada et al. [4] investigated the occurrence of water flooding in the gas diffusion layer (GDL) of a PEMFC, and their results showed that it was water flooding in the GDL that directly caused the concentration polarization. They also found that liquid water accumulated more rapidly under channel ribs with the increase in current density, because liquid water under ribs was harder to be expelled due to the longer transport route. Turhan et al. [12] studied liquid water buildup and distribution in a PEMFC using the neutron imaging method, and their results showed that liquid water buildup decreased with increasing inlet gas flow rate. They also showed that due to restricted mass

---

* Corresponding author. Tel.: +852 2358 8647; fax: +852 2358 1543.
E-mail address: metzhao@ust.hk (T.S. Zhao).

1388-2481/$ - see front matter © 2006 Elsevier B.V. All rights reserved.
doi:10.1016/j.elecom.2006.10.031

transport, there was liquid water under ribs even at very high flow rates and low humidity. Nguyen [21] designed the interdigitated flow field, with which gas was forced to flow through the GDL and the shear force of this gas flow helped blow out the liquid water that was entrapped in the inner layers of the electrodes. As a result, mass transport rates of the reactants from the flow channel to the inner catalyst layer could be improved, and the water flooding problem at the cathode could be significantly reduced. Williams et al. [24] experimentally found that convection under ribs also occurred in a serpentine flow field due to the pressure difference between two adjacent channels, and this convection improved oxygen transport and helped blow out liquid water in the GDL, reducing transport losses from flooding. Jang et al. [25] studied a baffle-blocked flow field, and found that gas convection in the GDL could be enhanced due to the baffle-blockage effect, which enhanced the reactant transport to the inner electrode and benefited water removal and flooding prevention.

Our literature review indicates that water flooding in the GDL under ribs is usually more serious than elsewhere at the cathode. The previous studies also demonstrated that channel-to-channel convection under ribs can facilitate both mass transport into the electrode and removal of water flooding. Therefore, enhancing convection through the GDL by optimizing the flow field is an effective way to reduce water flooding at the cathode, enhance the mass transport, and thus improve both cell performance and operating stability. Based on this understanding, we designed a new flow field for PEM based fuel cells, which was obtained by re-patterning conventional single serpentine flow fields. We showed theoretically that the new flow field induces enhanced gas flow through the GDL without increasing the compressor power. We applied this new flow field to an in-house fabricated DMFC and demonstrated the marked features of the new flow field over the conventional serpentine flow field design.

2. Theoretical

Consider a conventional single serpentine flow field (SFF), shown in Fig. 1a, in which one continuous channel that proceeds through a series of alternating 180° turns and 14 ribs with the same length of 29.0 mm are formed. When a fluid is pumped to flow through the channel from the inlet to the outlet, the local pressure in the channel can be approximated by:

$$P(x) = P_{\text{inlet}} - P_{\text{loss}}(x) = P_{\text{inlet}} - \frac{128\mu Q}{\pi D_{\text{eff}}^4}x \tag{1}$$

where Q is the mass flow rate of the fluid, D_{eff} is the effective dynamic diameter of the fluid flow, and x is the channel distance measured from the inlet [32]. Eq. (1) indicates that the pressure decreases with x downstream due to viscous losses, resulting in a pressure difference across each channel rib. For example, the pressure at point M (x_{M}) is higher than that at point N (x_{N}). It follows from Eq. (1) that the corresponding pressure difference across the rib, i.e., between points M and N, is given by:

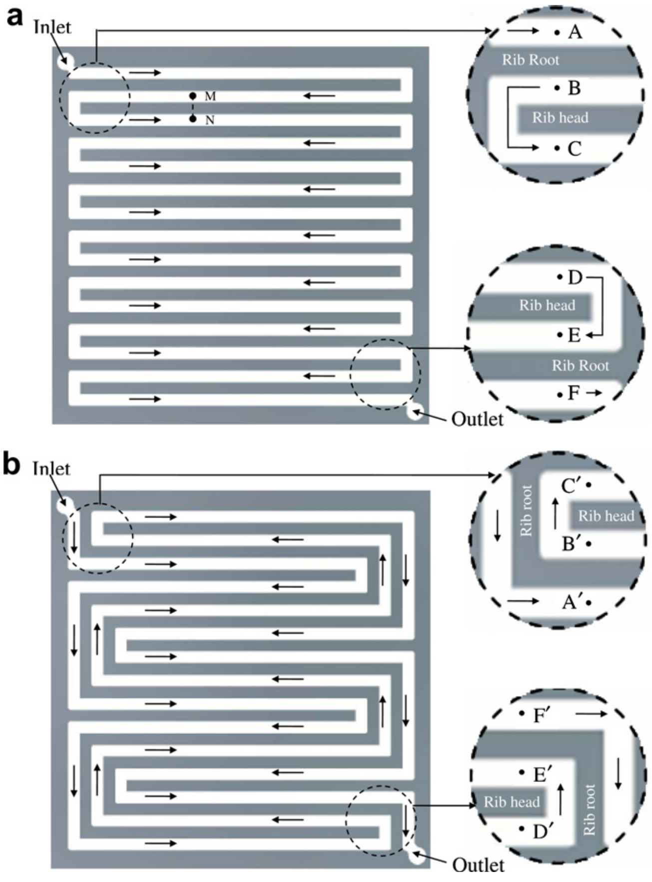

Fig. 1. Designs of the flow fields (drawn to scale) : (a) SFF and (b) CESFF.

$$\Delta P = P(x_{\text{M}}) - P(x_{\text{N}}) = \frac{128\mu Q}{\pi D_{\text{eff}}^4}(x_{\text{N}} - x_{\text{M}}) \tag{2}$$

This pressure difference tends to lead to an in-plane "short-circuit" flow through the porous GDL under ribs, referred to as under-rib convection hereafter [24,26–28], with its average artificial velocity represented by Darcy's law:

$$\mathbf{v} = -\frac{K}{\mu}\nabla P = \frac{128KQ}{\pi D_{\text{eff}}^4 W}(x_{\text{N}} - x_{\text{M}}) \tag{3}$$

where K is the fluid permeability through the GDL and W is the rib width. Eq. (3) indicates that for a given mass flow rate Q, the strength of under-rib convection between points M and N depends upon the geometric dimensions of channel and GDL, such as the rib width, W, and fluid permeability through the GDL, K. It is also clear from Eq. (3) that the strength of under-rib convection is not uniform, varying linearly from zero to the maximum value according to channel length x. We now show that the strength of under-rib convection near each rib head (see Fig. 1a) is nearly zero but it reaches a maximum near each rib root. We first look at the strength of under-rib convection in the channel inlet region (the upper-left corner). As illustrated in Fig. 1a,